Discrete element investigation of rate effects on the asymptotic behaviour of granular materials

David MAŠÍN [a,1] and Jan JERMAN [a]

[a] *Faculty of Science, Charles University in Prague, Czech Republic*

Abstract. The effect of loading rate on the asymptotic behaviour of a granular material with permanent particles is investigated using discrete element method. The asymptotic states could uniquely be represented in terms of dimensionless inertial number *I*. For low inertial numbers (*I* lower than 0.01 to 0.001), the asymptotic stress ratio is independent of *I* (and thus of loading rate and of mean stress). This agrees with observation on soils, showing critical state friction angle independent of mean stress. For low inertial numbers, the critical state line as well as the isotropic normal compression line have similar slope in the plane of void ratio vs. mean stress to the isotropic rebound line. This agrees with conclusions of other scientists, who suggest that particle crushing needs to be involved to represent more realistically the volumetric asymptotic response of granular material.

Keywords. Asymptotic states, rate effects, discrete element method, granular flow

1. Introduction

In this paper, we present a continuation of the work by Mašín [1], who studied asymptotic properties of granular materials using discrete element method (software Yade). Asymptotic states can be defined as states reached after sufficiently long proportional loading (loading with constant direction of stretching rate). They have been known from both experiments on granular materials and from numerical simulations. In fact, asymptotic states are incorporated in most of the soil constitutive models based on the critical state soil mechanics, including both the elasto-plastic and hypoplastic models (explicit incorporation of asymptotic states into hypoplasticity is described in [2],[3]).

To graphically illustrate the asymptotic states, we first define two stress and strain obliquity measures ψ_σ and $\psi_{\dot\epsilon}$ (Gudehus and Mašín [4]), see Fig. 1. The asymptotic state concept is then introduced in Fig. 2. Each of the strain rate directions $\psi_{\dot\epsilon}$ is associated with a single stress obliquity direction ψ_σ (Fig. 2a). In addition, each of the strain rate directions $\psi_{\dot\epsilon}$ is also associated with a unique asymptotic trace in the mean stress *p* vs. void ratio *e* plane, denoted as normal compression line (Fig. 2b). The two graphs can be combined into a three-dimensional object denoted as asymptotic state boundary surface, whose constant volume section is shown in Fig. 2c. Mašín [1] also defined asymptotic states in extension, in addition to the asymptotic states in compression shown in Fig. 2. The most important of all the asymptotic states, representing the state when the granular

---

[1] Corresponding Author.

material flows at constant volume (thus associated with $\psi_{\dot{\varepsilon}} = 90°$). It is traditionally denoted as *critical state* in soil mechanics.
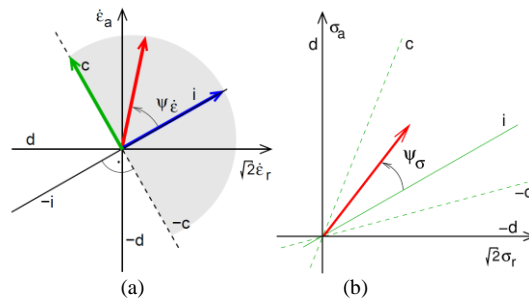

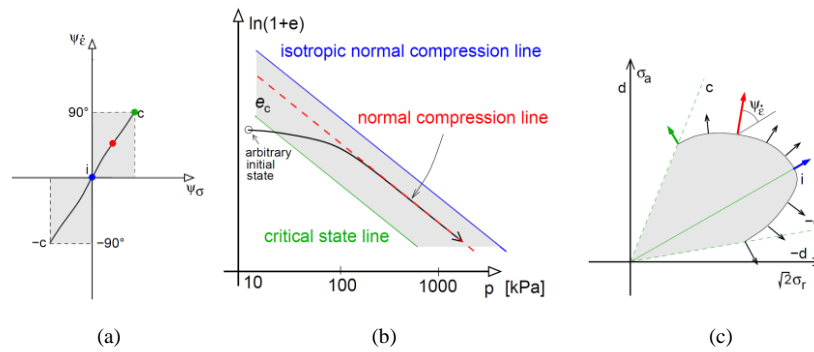**Figure 1.** Definition of angles $\psi_{\dot{\varepsilon}}$ and ψ_{σ}

Figure 2. Graphical representation of compression asymptotic states

The main conclusions of the work by Mašín [1] were as follows. First of all, he confirmed existence of asymptotic states, both in compression and in extension. He noted that the asymptotic states were predicted irrespectively of the fact the particles were elastic and spherical (thus non-crushable). He also observed that the asymptotic stress ratio (including the critical state friction angle) depended on the mean effective stress. This conclusion, differing from the known soil behaviour, was attributed to the loading rate, but no further investigation was done in this respect.

In the present paper, we continue the work by Mašín [1] by investigating of the rate effects on the asymptotic response of granular materials.

2. Dicrete element model

The charateristics of the discrete element model were identical to the model from [1]. It has been setup within dicrete element code Yade [5]. The particles were spherical and permanent with granulometry of a real sand (particle sizes ranging from 0.2 mm to 1 mm). To eliminate the influence of the model boundaries, periodic boundary conditions have been adopted, so that the modelled unit cell (as well as all its particles and all their

properties) is surrounded by identical cells shifted along the cell edges. A simple elastic-frictional contact law has been adopted with parameters E = 500 MPa, ν = 0.3 and φ = 0.5 Rad (coefficient of friction $\mu_{contact}$ = 0.546). The rolling resistance (rotational spring) was not considered. The sample was generated using an algorithm ensuring that they followed the prescribed particle size distribution, were randomly distributed, and were initially not in contact. The prescribed particle density was ρ_s = 2650 kg/m^3 and acceleration due to gravity was zero. The sample has first been compressed under isotropic conditions with constant value of the Euclidean norm of the Euler stretching tensor ||**D**|| up to different isotropic stresses. As in this work we focused on constant volume loading only, the sample was subsequently sheared (with the same value of ||**D**|| as used in compression) at a condition of $\psi_{\dot{\epsilon}} = 90°$. The influence of ||**D**|| was investigated.

The analyses by Mašín [1] have been performed with specimen consisting of 150000 spherical particles. This high number of particles ensured accuracy of the obtained response; it however also led to computationally demanding simulation, not feasible at much lower stretching rates investigated in this work. We thus first investigated the influence of the specimen size on the simulation results (Fig. 3; note that abbreviation [GM12] indicates the results from Mašín [1] throughout this paper). We observed that the response is not significantly affected by the specimen size for specimens with more than approx. 15000 particles. In this work, a sample consisting of 16700 particles has been used in the simulations.
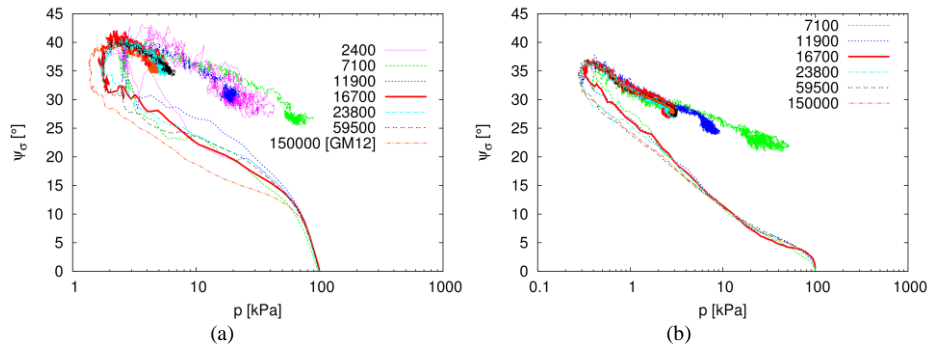

Figure 3. The influence of the specimen size on the simulation results ($\psi_{\dot{\epsilon}} = 90°$). Specimen with 16700 particles selected for rate-effects investigation. (a): rate 334 s^{-1} [GM12], (b) rate 33.4 s^{-1}.

3. Rate-effects on the asymptotic response

3.1. Rate effects for a single consolidation stress

In the first set of analyses, the specimens have been consolidated isotropically up the mean stress of 1000 kPa and sheared subsequently at $\psi_{\dot{\epsilon}} = 90°$ up to the asymptotic state (critical state) at various values of ||**D**||. Results are shown in Fig. 4, showing graphs for the $\psi_{\dot{\epsilon}} = 90°$ loading phase (Fig. 4a,c,d), and also for the isotropic compression stage (Fig. 4a, b).

Figures 4c,d show that decreasing the loading rate by almost 4 orders of magnitude decreases the asymptotic stress ratio and, concurrently, it also changes the stress path so

that the asymptotic states are with decreasing loading rate reached at progressively lower mean stresses. Interestingly, the curves at low loading rate show intermittent peak in the stress path (Fig. 4d), followed by an immediate mean stress decrease and subsequent increase of the stress ratio up to the asymptotic state. This behaviour will be discussed later in Sec. 4.
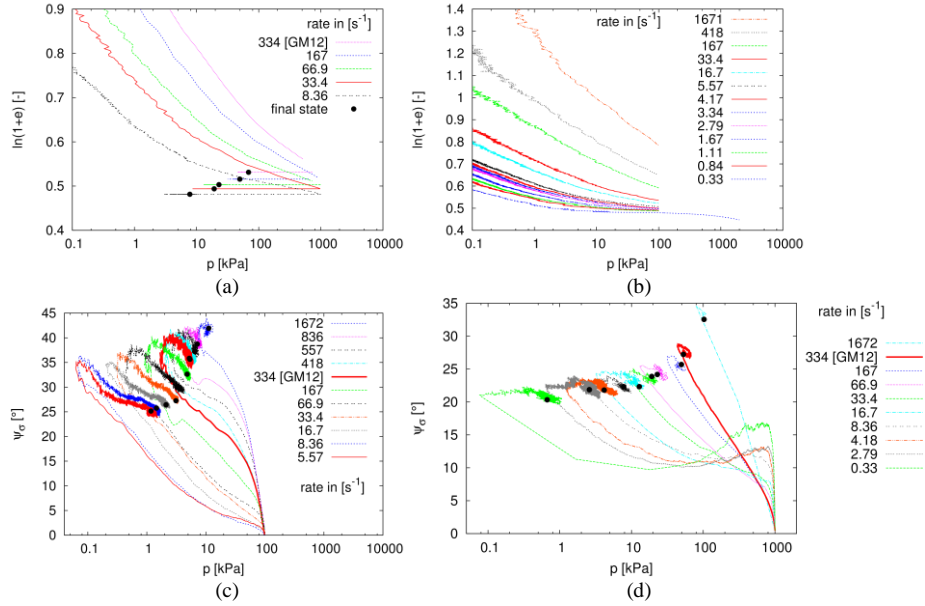

Figure 4. The influence of loading rate $\|\mathbf{D}\|$ on the asymptotic behavior for consolidation stress of 1000 kPa

Figure 4b shows that the loading rate affects not only the asymptotic stress ratio at constant volume, but it also affects the isotropic loading phase of the test, such that the isotropic normal compression lines are progressively lower in the effective stress vs. void ratio plane. In fact, for low loading rates the normal compression lines have small slope, such that there is not a significant difference between the compression and rebound line (rebound response not shown in Fig. 4 for clarity, however). This is consistent with findings by [6,7] and others, who suggested that to realistically model normal compression of soil-like material, particle breakage must be considered. Finally, Fig. 4a demonstrated that the final state of the constant volume shearing depends on shearing rate not only in terms of stress ratio, but also in terms of the asymptotic void ratio.

3.2. Asymptotic states for different consolidation stresses

In the subsequent set of analyses, we selected five different loading rates ($\|\mathbf{D}\|$=334s^{-1}, 33.4s^{-1}, 16.7s^{-1}, 2.79s^{-1} and 0.33s^{-1}) and studied the asymptotic response for different consolidation stresses (Fig. 5). Consistently with Fig. 4d, decreasing the loading rate increases a tendency to mean effective stress decrease in proportional loading. For fast loading, the stress ratio ψ_σ increases continuously and the asymptotic states align evenly along a well-defined asymptotic state line. For slower loading rates, however, different behaviour is observed. The samples compressed to lower stresses evince a sharp stress ratio decrease before reaching the asymptotic state. The asymptotic state is still well-

defined in the ψ_σ vs. mean stress plane, we can however distinguish two different data clusters. One cluster corresponds to samples compressed isotropically to high stresses. These samples reach the asymptotic state before the stress ratio decrease could have occurred and the asymptotic state is associated with high mean stresses. The second group of samples show a stress ratio decrease before they could have reached the asymptotic state, and consequently the mean stress at the asymptotic state is remarkably low.
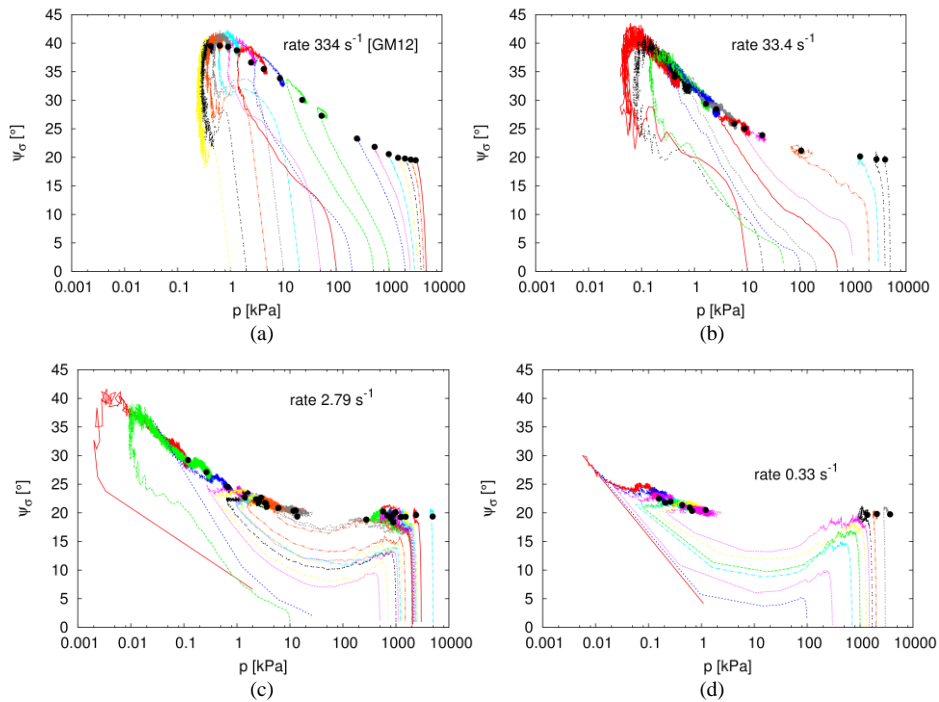

Figure 5. The influence of loading rate $\|\mathbf{D}\|$ on the asymptotic behaviour for different consolidation stresses

The asymptotic states from Fig. 5 are re-plotted in Fig. 6 for better demonstration of the loading rate effects. A decreased loading rate decreases the dependency of the asymptotic stress ratio on mean stress (Fig. 6a). This leads us to hypothesis that for low loading rates the asymptotic stress ratio would be independent of the mean effective stress: consistently with the known behaviour of soils, where the critical state friction angle is generally assumed to be independent of the stress level. More discussion on this fact is given in Sec. 4. Figure 6b shows that not only the stress ratio, but also the void ratio at the asymptotic state depends on the loading rate (decreasing loading rate implies decreasing asymptotic void ratio). This has already been observed in Fig. 4a.
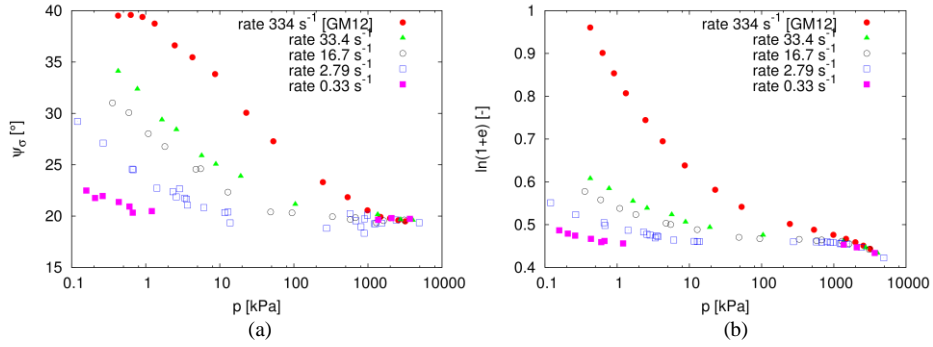
Figure 6. Asymptotic states for different loading rates plotted in p vs. ψ_σ (a) and p vs. e (b) planes

4. Dimensionless analysis

Dimensionless quantities proved to be a powerful unifying reference for representation of granular flows. It has been observed by various authors [8][9], that the coefficient of friction μ^* of a granular assembly can be uniquely represented in terms of so-called *inertial number* I, which has been for general loading case defined by Jop et al. [10] as

$$I = \|\mathbf{D}\| d \sqrt{\frac{2\rho_s}{p}} \tag{1}$$

The coefficient of friction μ^* was found to be independent of *I* for values of inertial number lower than approx. 0.01 [8][9]. For higher inertial numbers, the coefficient of friction increased with increasing *I*.

Figure 7 shows values of the inertial number of the three loading rates investigated. Two lines are plotted for each loading rate, the higher one corresponds to the largest particle within the system (d=1 mm) and the lower one for the smallest particle within the system (d=0.2 mm). The threshold value of *I*=0.01 is also plotted for indication. If the asymptotic stress ratio was to depend on *I* with the threshold value of *I*=0.01, it would be expected from Fig. 7 that the specimen loaded at $\|\mathbf{D}\|$=0.33s⁻¹ would evince the asymptotic stress ratio practically independent of mean effective stress. The other two loading rates would lead to the asymptotic stress ratio dependent on *p*.
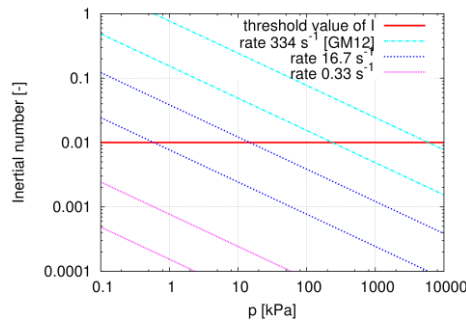

Figure 7. Inertial number *I* plotted for the three loading rates investigated. The higher line corresponds to the largest particle size (d=1 mm), whereas the lower line to the smallest particle size (d=0.2 mm).

A graph showing directly the dependency of the asymptotic states on the inertial number is in Fig. 8 (plotted for *I* calculated for the largest particle within the system, that is for d=1 mm). The dependency of the asymptotic stress ratio ψ_σ on *I* is shown in Fig. 8a. All the available data align along a curve in the ψ_σ vs. *I* plane. Still, however, the curve is not unique and some rate-dependency is observed. This indicates that the dimensionless analysis using the inertial number is valuable not only for the representation of friction coefficient in the simple shear test, but it is representing the asymptotic behaviour in general. The limiting inertial number separating the quasi-static and the dynamic regimes is between approximately *I*=0.001 and *I*=0.01. Figure 8c shows the same data re-plotted in terms of coefficient of friction μ^*.
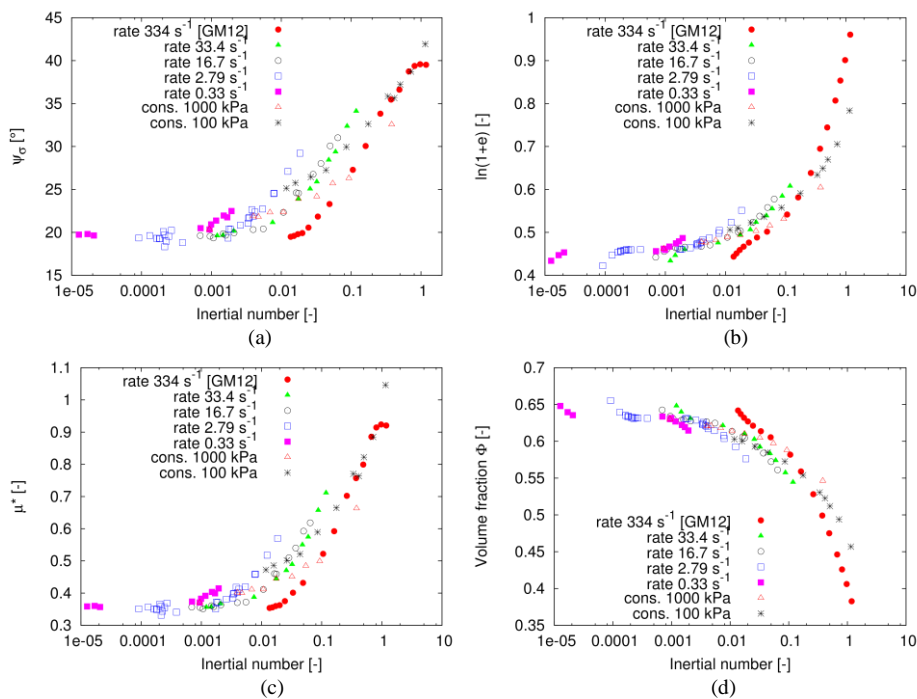

Figure 8. Asymptotic state for $\psi_{\dot\varepsilon} = 90°$ represented in terms of the dimensionless inertial number *I*.

Similarly to the stress ratio, also the void ratio vs. *I* relationship depends on the inertial number (Fig. 7b). For low inertial numbers the slope of the e vs. *I* curve is very low, similar to the isotropic rebound line (not shown here). Note that the apparent steep tails of the e vs. *I* dependencies at low inertial numbers are caused by non-negligible particle overlaps, which is a side-effect of the discrete element method simulation procedure (see [1] for the particle overlap quantification). The same data are re-plotted in Fig. 7d in terms of volume fraction ϕ, defined as a ratio of volume of particles and the sample volume.

It is to be pointed out that while the void ratio vs. *I* at asymptotic state relationship is remarkably flat at low inertial numbers (the slope not being substantially different from the isotropic rebound modulus, see [1]). This explains the tendency of the system to the

sharp decrease of the stress ratio before reaching the asymptotic state observed above (Fig. 5). $\psi_{\dot{\varepsilon}} = 90°$ loading is, by definition, characterized by constant void ratio. The samples consolidated to higher void ratios must show remarkable mean stress decrease during asymptotic loading to reach the asymptotic state; contrary, the samples consolidated to lower void ratios (caused mostly by particle overlap) would remain at high mean stresses at the asymptotic state. As the void ratio vs. I curve is flat for low inertial numbers, the gap between the two modes of behaviour is very narrow and finally the data show two distinctive clusters (Fig. 5).

5. Concluding remarks

In the paper, we investigated the effect of loading rate on the asymptotic behaviour of granular material using discrete element method. Among different asymptotic states, we selected constant volume proportional loading for our investigation. We have shown that the asymptotic stress ratio and void ratio can be represented in terms of dimensionless inertial number I. For I lower than 0.001 to 0.01, quasi-static regime with constant asymptotic stress ratio has been observed, which agrees with the known behaviour of soils (critical state friction angle independent of mean stress). For low inertial numbers, the normal compression lines are remarkably flat. This agrees with conclusions of other scientists who suggest that particle crushing needs to be involved to represent more realistically volumetric asymptotic response. For higher inertial numbers, both the stress ratio and asymptotic void ratio depend on I.

Acknowledgement

References

[1] Mašín D., Asymptotic behaviour of granular materials. *Granular Matter* **14** (2012), 759–774.

[2] Mašín, D. Hypoplastic Cam-clay model. *Géotechnique* **62** (2012), 549–553

[3] Mašín, D., Clay hypoplasticity with explicitly defined asymptotic states. *Acta Geotechnica* **8** (2013), 481–496.

[4] Gudehus, G. and Mašín, D., Graphical representation of constitutive equations. *Géotechnique* **59** (2009) 147–151.

[5] Šmilauer, V., Catalano, E., Chareyre, B., Dorofenko, S., Duriez, J., Gladky, A., Kozicki, J., Modenese, C., Scholtès, L., Sibille, L., Stránský, J., Thoeni, K.: Yade Documentation, 1st edn. *The Yade Project* (2010). http://yade-dem.org/doc

[6] Cheng,Y.P.,Nakata,Y.,Bolton, M.D, Discrete element simulation of crushable soil. *Géotechnique* **53** (2003), 633–641.

[7] McDowell, G.R., Bolton, M.D., On micromechanics of crushable aggregates. *Géotechnique* **48** (1998), 667–679.

[8] da Cruz, F., Emam, S., Prochnow, M., Roux, J.N., Chevoir, F, Rheophysics of dense granular materials: discrete simulation of plane shear flows. *Phys. Rev. E* **72** (2005), 021309.

[9] Hatano, T., Constitutive law of dense granular matter. *J. Phys.: Conf. Ser.* **258** (2010), 012006.

[10] Jop, P., Forterre, Y., Pouliquen, O., A constitutive law for dense granular flows. *Nature* **441** (2006), 727–730.